

V/V_{max} Statistics and Neo-Classic Cosmological Tests

L. Van Waerbeke¹, G. Mathez¹, Y. Mellier¹, H. Bonnet¹, M. Lachièze-Rey²

¹ Laboratoire d'Astrophysique de Toulouse, URA285. Observatoire Midi-Pyrénées 14, avenue Edouard Belin F-31400 - Toulouse

² CEN Saclay Service de Physique Théorique F-91191 Gif Cedex

Received ; Accepted

Abstract. A new cosmological test is derived, based on the distribution of individual V/V_{max} in a complete redshift-limited sample of distant objects. The fundamental assumption is that, in any range of absolute luminosity, individual V/V_{max} are required to be uniformly spread over the $[0, 1]$ range. Under the assumption of Pure Luminosity Evolution, this gives rise to a natural partition of the sample into *high luminosity, redshift-limited* and *low luminosity magnitude-limited* quasars. The behavior of V/V_{max} versus evolution and cosmology differs substantially in the two subsamples. This condition of uniformity is probed in any absolute magnitude bin, allowing a likelihood function to be computed from the Kolmogorov–Smirnov probabilities of each bin. Monte–Carlo simulations show that the test is mostly sensitive to the density parameter, but, under certain conditions, it also sets constraints on the space curvature and, to a lower extent, on the cosmological constant. The efficiency of this test applied to two kinds of simulated quasar samples is examined: large number QSO sample, but limited to redshifts $z < 2.2$ or smaller in QSO number, but with higher a redshift limit. Power law and exponential luminosity evolution laws are compared, and cross–tests show that the functional form of luminosity evolution does *not* affect substantially the probabilities in the parameter space (Ω_{mat}, Λ) . The test is then applied to the UVX sample of Boyle et al. (1990). A low matter density, and a flat Universe without cosmological constant, are rejected: $0.2 < \Omega < 0.8$ within the 95 % confidence level.

Key words: Cosmology: observational tests; Quasars: evolution

1. Introduction

At the end of the sixties, the discovery of quasars was a promising tool for cosmology. In particular $\langle V/V_{max} \rangle$, originally designed to test the spatial uniformity of a stellar population, was used as a cosmological test. This test was expected to reject all of the 'bad' cosmologies where the average $\langle V/V_{max} \rangle$ differs significantly from 1/2. The first application to quasar samples lead to $\langle V/V_{max} \rangle$ significantly above 1/2 (Schmidt 1968), *whatever the assumed cosmology*. This finding was interpreted either in terms of a strong *Density Evolution (DE)* (Schmidt 1972), or in terms of *Luminosity evolution* (Mathez

1976, 1978). The $\langle V/V_{max} \rangle$ test is still the clearest evidence for quasar evolution (however, see Bigot and Triay 1991).

The situation soon appeared to be quite hopeless for the cosmological tests with QSOs: whatever the cosmology, whatever the nature and the functional form assumed for evolution, there exists a value of the characteristic evolution parameter ensuring $\langle V/V_{max} \rangle = 1/2$ within the statistical errors. In spite of many attempts, no reliable theoretical evolutionary model has been derived so far from the physics of quasar emission. Consequently, the study of evolution remains essentially phenomenological. Several papers followed similar procedures (Schmidt 1972; Mathez 1976; Marshall *et al.* 1983) in order to associate a value of the evolution parameter to a given cosmology. Turner (1979) proposed a slightly different way to perform magnitude-redshift tests with quasars. A Luminosity Dependent DE model (LDDE) was also proposed (Green et Schmidt 1983); this model however requires more data because it depends on two parameters at least. Applying $\langle V_e/V_a \rangle$ tests (in the sense of Avni and Bahcall 1980) to a composite sample of 300 objects, Kassiola and Mathez (1991) found that no single parameter evolution law (neither DE nor LE) gives complete satisfaction. This was probably due to sample inhomogeneity, since (Boyle *et al.* 1987,1990) found that a single, large, complete sample of 400 UVX QSOs is consistent with *Pure Luminosity Evolution (PLE)*.

Several new cosmological tests using QSOs have been recently proposed. Schade and Hartwick (1994) assume a functional form for LE and perform the Loh–Spillar test with QSOs (Loh and Spillar 1986). Deng *et al.* (1994) find a typical scale of the order of 100 Mpc in the spatial distribution of QSOs, and derive a cosmological test by comparing it to preferred scales in the galaxy spatial distribution (Broadhurst *et al.* 1990). However there is no clear consensus on this subject, since Shanks and Boyle (1994) also claim to detect significant correlation, but on scales one order of magnitude smaller. Phillipps (1994) applies a test originally proposed by Alcock and Paczynski (1979) to measure the cosmological constant from the mean projection angle between quasar-quasar separation and the line of sight. Finally Malhotra and Turner (1995) study the evolution of quasars in cosmological constant dominated flat universes.

This paper is the first of a series related to a new cosmological test using a neo–classical $\langle V/V_{max} \rangle$ approach. The motivation was to address the problem of evolution of QSOs in non-zero Λ cosmologies, where evolution should be less. (Mathez *et*

Send offprint requests to: L. Van Waerbeke

al. 1995, Paper II) Previous analyses did not consider this case, except one paper (Malhotra and Turner 1995). However, some recent determinations of the Hubble constant from HRCam images (Pierce *et al.* 1994) or HST images (Freedman *et al.* 1994) give high values of H_0 incompatible with the age of globular clusters, unless $\Lambda > 0$ (see e.g. the discussion in Leonard and Lake 1995). On the other hand, the statistics of multiply imaged QSOs (Kochanek 1990; Helbig *et al.* 1995), as well as galaxy number counts from Yoshii *et al.* (1995) provide an upper limit on Λ , which seems lower than 0.9. If it is confirmed that $\Lambda > 0$, then the discrepancy between the vacuum energy of physicists and the cosmological constant of astrophysicists could be a severe problem for standard physics. The alternative theory of Scale Relativity (Nottale, 1993) which introduces $\Lambda^{-1/2}$ as a natural limiting length analogous to the velocity of light in Special Relativity, should be explored seriously.

The present paper is exclusively concerned with PLE, and a forthcoming paper will be devoted to PDE.

In Section 2, the basic ideas of the test and the fundamental hypotheses on QSO statistics are given. In Section 3, we show how to associate a probability to a cosmological model. In Section 4, we derive the expression of V/V_{max} suited for the brightest quasars. Catalogues are produced with Monte-Carlo simulations in Mathez *et al.* 1995, (hereafter Paper II). The test is applied to these catalogs in Section 5, and on a real QSO catalogue in Section 6. The main results are discussed in the last Section, where the hypotheses are summarized.

2. Distribution of Maximum Volumes in a Complete Sample

2.1. The spirit of the test

Our working frame is the Friedmann-Lemaître cosmologies. The QSO Luminosity Evolution is described, as usual, by a given functional form depending on a single evolution parameter. Our null hypothesis is that the QSOs are uniformly distributed in volume, and that we deal with a sample complete in magnitude. To properly account for the well known observational biases present in complete QSO samples at low and high redshifts, one has to work in a restricted redshift range. The variable which is uniformly distributed is not V/V_{max} , but a ratio x defined in Section 4. The sample is binned according to M_0 , the absolute magnitude defined at the epoch $z = 0$ and at the frequency where observations are done. Since in the frame of the correct model (evolution and cosmology) the x distribution does not depend on the absolute magnitude, each bin must have a uniform x distribution. A correlation between V/V_{max} and absolute magnitude is one of the most sensitive pieces of evidence for a wrong choice of cosmology and/or evolution (see Fig. 1 and Bigot and Triay 1991). Fig. 1 shows the positions of QSOs in the $(M_0, V/V_{max})$ plane for three values of the evolution parameter. A study of the V/V_{max} distribution is clearly less sensitive in the whole sample than in luminosity bins.

Another interesting piece of information is the evolution of individual x versus the cosmology and the evolution characteristic parameters (see Fig. 2). We expect that a cosmological test using the x values might be mostly sensitive in the regions of parameter space where x vary strongly. As we see in Fig. 2, two asymptotic regions, toward $\Lambda < 0$ and $\Omega_{mat} > 1$, are observed, which show that the test will be insensitive to the cosmology in these regions.

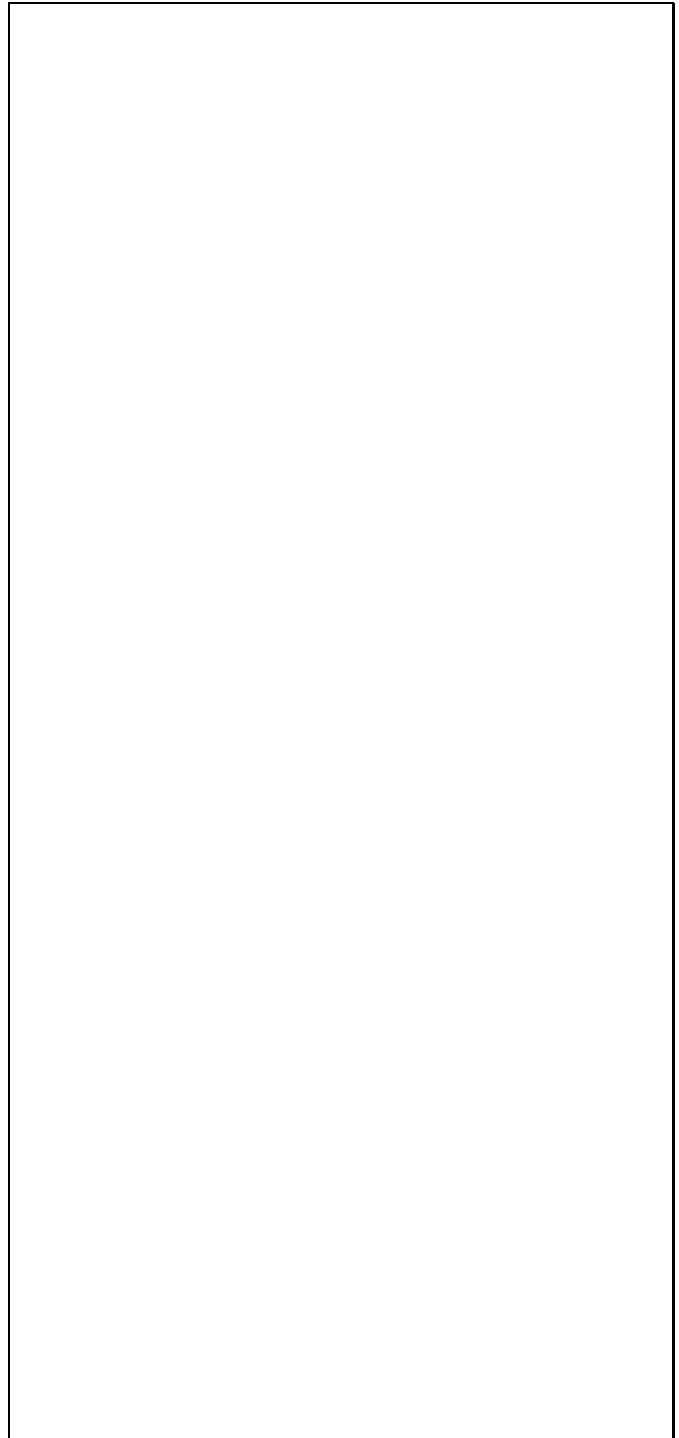


Fig. 1. The basic idea of the test: Boyle's *et al.* (1990) QSOs are represented in the (absolute magnitude- V/V_{max}) plane. The model is power law luminosity evolution (PWLE), $\Omega = 1, \Lambda = 0$. The values of the evolution parameter are $k_L = 0., 3., 6.$, respectively. The upper and lower plots show a strong correlation, corresponding to a bad combination of evolution and cosmological model. In the middle, there is no correlation whatever the magnitude. It can be seen that the *global* $\langle V/V_{max} \rangle$ may be 1/2, while the distribution is far from uniform in the high- and low-luminosity bins.



Fig. 2. V/V_{max} ratio versus cosmological parameters for 15 QSOs randomly chosen in the Boyle’s *et al.* (1990) sample. Top left, $\Lambda = 0$, top right, $\Lambda = 1$, bottom left, $\Omega_{mat} = 1$, bottom right, $\Omega_{mat} = 2$. The evolution parameter always corresponds to the maximum likelihood. Discontinuities in the derivative correspond to change of status from magnitude– to redshift–limited or conversely. Noise in the bottom curves is due to computational difficulties. In the two asymptotic regimes discussed in text (towards large Ω and small Λ), the test has little or no sensitivity, while the test is quite efficient at low Ω .

2.2. Luminosity Evolution

Pure Luminosity Evolution has been introduced in a phenomenological way, without physical support. It corresponds to the case where the fraction of active galaxies is constant versus redshift, but not their luminosity. Although it is a statistical evolution of the whole population, the usual simplifying hypothesis on luminosity evolution is that *all* quasar absolute luminosities L do evolve in parallel according to the law (Mathez 1976, Marshall *et al.* 1984, Boyle *et al.* 1987):

$$L(t(z)) = L(t_0) \times e(t(z)), \quad (1)$$

where $e(z)$ has either the ‘power law’ form in the PWLE case:

$$e(z) = (1+z)^{k_L}, \quad (2)$$

or the ‘exponential’ form in the LEXP case:

$$\begin{aligned} e(z) &= \exp[(t_0 - t(z))/\tau] \\ &= \exp[k_L H_0 (t_0 - t(z))]. \end{aligned}$$

$t(z)$ is the cosmological epoch corresponding to redshift z , $t_0 = t(z=0)$, $\tau = 1/(k_L H_0)$ is the characteristic evolution time, and k_L , the ‘evolution strength’ in the standard notation.

2.3. Evolutionary tracks in the Hubble plane

Several pairs of independent variables may be used to study the quasar distribution: redshift, volume, and comoving volume

on one hand and apparent magnitude, flux density, intrinsic luminosity on the other hand. Here we prefer to work in the Hubble plane, apparent magnitude–redshift (m, z), because it corresponds to observables. No hypothesis either on cosmology or on evolution are needed to represent quasars in this plane.

Assume that we have a quasar sample complete in the magnitude range $[m_1, m_2]$, in a given sky area. The fainter limit m_2 is obvious. The bright limit m_1 may arise from photometric saturation (either in the photometric or in the spectroscopic data). Quasars of the sample thus lie inside what we call ‘box \mathcal{B} ’ in the following, i.e. the domain $[m_1, m_2] \otimes [z_1, z_2]$ of the Hubble plane: we further restrict ourselves to some range of absolute magnitude $[M_0^1, M_0^2]$, arbitrary provided that $[M_0^1, M_0^2] \otimes [z_1, z_2]$ is included in box \mathcal{B} .

According to Eq. 2, all quasars follow parallel evolutionary tracks in the Hubble plane. Now consider a given quasar in box \mathcal{B} . Its evolutionary track will go along the $m(z)$ curve in the Hubble plane, described by the Mattig relation:

$$m(z) = M_0 - 5 + 2.5 \log_{10} (d_L(z)^2 \times K(z)/e(z)) \quad (3)$$

where M_0 is the absolute magnitude at epoch $z=0$, $d_L(z)$ is the luminosity distance and $K(z)$ is the K–correction: $K(z) = (1+z)^{\alpha-1}$ with $\alpha = 0.5$ as spectral index. Note that in the case of a strong luminosity evolution, the $m(z)$ relation is no longer monotonic, and can even exhibit several local maxima in some extreme cases. It is necessary to exclude for any volume computation, all the redshift ranges where $m > m_2$ or $m < m_1$ (see the details in Paper II). The stronger the evolution, the smaller will be the slope of the evolutionary track. It can become negative if evolution is such that apparent magnitude passes through a maximum. Fig. 3 shows one illustration of the Mattig relation when the evolution is stronger than the cosmological extinction.

2.4. Observational cutoffs at low and high redshift

As has been known for a long time, the redshift distribution of most large complete QSO samples is biased at low and high redshift. These cutoffs are important to account for, since they govern the locus of both extremities of evolutionary tracks in the Hubble plane.

At low redshift, it is easier to distinguish the host galaxy of QSOs, so many of them *do not* have a stellar appearance and are missed in quasar samples. We will restrict our analysis to redshifts $z > 0.3$.

Searching for ultraviolet excess (UVX) stellar objects is the most efficient way to detect quasar candidates, so the largest complete samples consist of UVX quasars. At high redshift, quasars no longer have any ultraviolet excess, since Ly_α , the dominant emission line, passes to the blue filter at $z \simeq 2.3$. So most of the large quasar samples are in fact limited to $0.3 < z < 2.2$. To our knowledge, Kassiola and Mathez (1991) and Crawford (1995) are the first authors to explicitly mention that using maximum or minimum redshifts outside the range $[0.3, 2.2]$ for UVX QSOs is erroneous. In Paper II, the joint distribution of redshift and magnitude is examined in the frame of PLE, and it is shown how to compute the individual ratios x which are uniformly distributed over $[0, 1]$ for quasars in any arbitrary bin of absolute magnitude.

In the next Section, we will take advantage of these properties to derive a cosmological test.



Fig. 3. Various Mattig functions with different absolute magnitudes, show parallel evolutionary tracks in the Hubble plane. Between the separators \mathcal{S}_∞ and \mathcal{S}_∞ , all QSOs are redshift-limited. The sign + on the bottom line denotes a QSO whose redshift z is limited in the range $[z_{min}, z_{max}]$ because of the bright magnitude limitation $m < m_1$.

3. Maximum Volume and Minimum Entropy

Our improved V/V_{max} analysis, essentially based on the Kolmogorov-Smirnov test, is somewhat similar to that used in the study by Zieba and Chyzy (1991) of high- and low-redshift radio galaxies. We show with details hereafter how it enables us to associate a significance level to each cosmological model and to reject some of them.

3.1. Choosing a grid of cosmological models

Most of the previous cosmological tests have been performed under the assumption $\Lambda = 0$, with either a low density parameter Ω_{mat} or a flat universe $\Omega_{mat} = 1$ (Ω_{mat} is the total density parameter, including baryonic and non-baryonic matters). Some tests however adopt a non zero cosmological constant but impose a null curvature by the condition $\Omega_{mat} + \Lambda = 1$. Present ideas on the density parameter are synthesized in Table 4. To explore a large range of cosmological models, we choose the range $[0, 3]$ for Ω_{mat} , and $[-1, 2]$ for Λ , varying these parameters independently, by steps of 0.2. However we exclude from the test all cosmologies without an initial singularity (see Carroll *et al.* (1992) for details). It results in $16 \times 16 - 17 = 239$ cosmological models. Absolute magnitudes are irrelevant in the test, only the rank of these magnitudes is important, which is independent of H_0 . Our test, based on the statistics of individual V/V_{max} ratios, is *totally independent* of the Hubble parameter.

3.2. Associating a confidence level to each cosmological model

We work in the (*absolute magnitude* – V/V_{max}) plane. We choose a functional form of the evolution before performing the test. Our test consists in ensuring a maximum likelihood

to the null hypothesis of *uniform distributions* of the x ratio defined in Section 4 *jointly in all bins of absolute magnitude*. We have to ensure this *without any hypothesis on the functional form of the luminosity function*.

Let \mathcal{M} be the current cosmological model (Ω_{mat}, Λ). To assign a probability to \mathcal{M} , we proceed as follows: once a value of the evolution parameter k_L is chosen, each ratio x is computed. The sample is ordered by increasing absolute luminosity and divided into n luminosity bins containing equal numbers of quasars. This is to minimize the noise that would be caused by very different numbers of quasars in each bin. In each luminosity bin we calculate the Kolmogorov-Smirnov probability that the corresponding x ratios come from a uniform distribution (see Press *et al.* 1992). Let $P_{KS}^i(\mathcal{M}, k_L)$ be this probability for the luminosity bin i . These bins are statistically independent, so are the probabilities, thus we can compute the likelihood function of the total sample of x :

$$\mathcal{L}(\mathcal{M}, k_L) = \prod_{i=1}^N P_{KS}^i(\mathcal{M}, k_L) \quad (4)$$

This likelihood is used to calculate an entropy:

$$\mathcal{E} = -2 \log(\mathcal{L}) \quad (5)$$

For each model \mathcal{M} , we determine the parameter k_L giving the lowest value of the entropy $\mathcal{E}_{low}(\mathcal{M})$. $\mathcal{E}_{low}(\mathcal{M})$ is defined as the entropy of the cosmological model \mathcal{M} . This operation is repeated for the 239 cosmological models to get an entropy map. At the end, the entropy is $\mathcal{E}_{low}(\mathcal{M}) = \mathcal{E}_{min} + \Delta\mathcal{E}(\mathcal{M})$, where \mathcal{E}_{min} is the lowest entropy found in the cosmological grid. $\Delta\mathcal{E}$ follows a χ^2 statistic with three degrees of freedom (Lampton *et al.* 1976), since three parameters are determined. For three parameters, the confidence intervals around the best model \mathcal{M} are given by $\Delta\mathcal{E} = 6.25, 7.80, 11.30, 16.20$ for the 90%, 95%, 99%, 99.9% confidence level respectively.

3.3. Choice of binning

The absence of an *analytical form of the luminosity function* has the drawback of preventing the use of a 2D Kolmogorov-Smirnov test in the ($M_0, V/V_{max}$) plane. So we are obliged to work in n luminosity bins and an arbitrary binning is substituted for an arbitrary analytic luminosity function. It is easier however to explore all the possible binnings than to explore all the possible analytic expressions! Moreover, the binning procedure is well suited to the method, which applies whatever the choice of the bin $[M_0^1, M_0^2]$.

In principle, the choice of the binning is not constrained. However, two practical limitations arise:

- As noted by Lampton *et al.* (1976), we should not proceed to reject some values of the cosmological parameters from confidence levels without a preliminary good fit cosmological model. This is equivalent to requiring that the lowest entropy \mathcal{E}_{min} of the most probable cosmological model not exceed $n - 3$ by much too much. This problem arises with too large n .
- The x ratio is calculated from the fictitious redshift displacement of a QSO according to the evolution law. However it must not be forgotten that the evolution law has only a statistical sense, and that it applies only to a QSO *population*. If the number of QSOs per bin is too small (i.e. if n is too large), the statistical sense of the evolution law is lost and the probability

map becomes noisy. We choose a bin number which keeps the smooth appearance of the probability map.

The method is validated by the analysis of synthetic quasar catalogues which are described in Paper II. By trial and error based on varying the size of the simulated QSO sample (see Section 5, Fig. 7), we found that the best choice from the point of view of the minimum entropy is to take approximately between 10 and 20 bins.

Since a large part of the work is made with these catalogues, we discuss them in Section 5.

4. How to compute V/V_{max}

4.1. Behaviour of x versus the parameters

In Paper II are introduced the various quantities necessary for computing the individual x ratios in a complete QSO sample. Two curves in the Hubble plane, the bright and the faint separators \mathcal{S}_1 and \mathcal{S}_2 , are of particular importance. These curves, shown in Fig. 3, delimit the domain \mathcal{D} , lying between them, and the domain \mathcal{D}^* which is its complementary with respect to box \mathcal{B} , or $[m_1, m_2] \otimes [z_1, z_2]$. All quasars in domain \mathcal{D} (here after \mathcal{D} quasars) are redshift-limited, while all \mathcal{D}^* quasars are magnitude-limited.

According to Paper II, the x ratio is uniformly distributed in the range $[0, 1]$ for quasars in any absolute magnitude range $[M_0^1, M_0^2]$. The x ratio takes quite a simple form for \mathcal{D} quasars:

$$x = \frac{V - V_1}{V_2 - V_1} \quad (6)$$

where the volumes $V_i = V(z_i)$ ($i = 1, 2$), the comoving volumes out to redshift z_i , are determined only from the cosmological model. For \mathcal{D}^* quasars, on the contrary, there are many different cases according to the respective values of z_1 and z_2 and of the redshifts where the magnitude equals one of the limiting magnitudes. An example is given in Fig. 3. Consider the QSO denoted by +. If we exclude from the volume computation the two redshift ranges where $m(z) < m_1$, then the x ratio for this QSO is:

$$x = \frac{V - V_{min}}{V_{max} - V_{min}}, \quad (7)$$

It should be noticed that k_L does not enter Eq. 6. k_L concerns \mathcal{D} quasars only inasmuch it governs the repartition of quasars with respect to the separators. On the contrary, V_{min} and/or V_{max} which enter the equivalent of Eq. 6 for \mathcal{D}^* quasars, do depend *explicitely* on k_L .

As evidenced in Fig. 2, the run of individual x ratios versus cosmological parameters varies substantially from quasar to quasar, although k_L is fitted to the maximum likelihood in each cosmological model of Fig. 2. Large variations and even inversion of slope correspond to the transition from one class to the other (magnitude- or redshift-limited). As Ω_{mat} increases at fixed Λ , and as Λ decreases at fixed Ω_{mat} , the curves tend towards horizontal asymptotes so it becomes impossible to test between various low Λ or high Ω_{mat} universes. However we will introduce in the following an alternative method based on the synthetic catalogues analysis to avoid this problem.

4.2. Towards efficient cosmological tests

Our method is far more demanding than a *global application* of the $\langle V/V_{max} \rangle$ test. We have several distinct sub-samples (the N absolute magnitude bins), which are independent in the sense that they do *not* contain the same objects and their x ratios do not behave similarly, neither with respect to evolution strength, nor with respect to cosmological parameters. The x -uniformity puts in N constraints instead of a single one: in some cosmological models, whatever the value of k_L , all the distributions of x ratios have too low a probability to be uniform *simultaneously* for all the absolute magnitude bins. This is exactly what is needed to reject some cosmological models as incompatible with a given hypothesis on quasar evolution.

One shortcoming of this test is that the evolution hypothesis itself may be wrong, although it is quite widely used. However the values of individual x ratios for \mathcal{D} quasars do not depend on the form and the value of the luminosity evolution and only depend on the cosmology. *If* there the proportion of \mathcal{D} quasars is sufficient in current samples then we will find some common results, even when varying the various evolution hypotheses. We will see in Section 6 that this is roughly the case.

There are various ways to perform the test: the redshift range $[z_1, z_2]$ may be divided into bins. There is presumably an optimal way to operate this redshift binning: since most of the effects of the cosmological constant are noticeable at high redshift, say $z > 1$, the essential contribution of the range $[0.3, 1]$ is likely to increase the noise. On the other hand the effects of varying Ω_{mat} are already noticeable at lower redshift (Carroll *et al.*, 1992), so that one can expect to get constraints on Ω_{mat} from the low redshift bin and constraints on Λ from the high redshift bin. There is probably an optimal compromise for the cutoff to be found somewhere around $z = 1$. In Section 6.1 we use this idea to apply the test to low redshift ($0.3 < z < 1.5$) and high redshift ($1.5 < z < 2.2$) samples of the Boyle QSO sample.

5. Monte-Carlo Simulations

5.1. Construction of Monte Carlo catalogues

Before applying the test on real data, we checked its efficiency on simulated samples. This is the only way to vary the cosmological parameters, or to search for the effect of the sample size, or of various biases in the redshift distribution.

We generated Monte-Carlo samples of 400 objects for each of the cosmological models of the grid defined above, and we analysed the simulated samples exactly as we did with Boyle's one. To simulate the catalogues, the procedures are the following:

- choose a model (cosmology + evolution functional form)
- determine the function $\Phi(M_0)$ from the Boyle *et al.* global luminosity function.
- given a limiting magnitude and an absolute luminosity, compute the available volume $V_a(M_0)$
- sort in luminosity according to the observed probability distribution function of luminosities in a sample, that is the product $\Phi(M_0) \times V_a(M_0)$
- given $V_a(M_0)$, sort in redshift ensuring homogeneous spatial distribution.

The last two steps are repeated once per object in the sample. All the details are described in Paper II.

5.2. Application of the test to simulated catalogues

In this Section we give the results of the test on various simulated catalogues by varying different parameters and by introducing some bias to understand how the test works. We choose to represent the contours at 90, 95, 99, 99.9% confidence levels which are the minimum confidence levels to reject some models. PWLE refers to power law luminosity evolution, and LEXP to exponential luminosity evolution. The limiting magnitude of the simulated catalogues is always $m_{lim} = 21$. No bright limit is set, since it complicates the computations and does not change the test.

5.3. Comparing parent cosmologies

Figs. 4 give the probability maps obtained in the (Ω_{mat}, Λ) plane for 5 different parent cosmological models. All maps correspond to samples of 400 objects with the same Monte-Carlo seed. All catalogues have been generated under the PWLE assumption, nevertheless varying the functional form of the evolution does not modify significantly the form of the contour maps. A large part of the parameter space is rejected with the models at low Ω_{mat} . This is expected from the Fig.2 because the stronger variations of the x ratios are precisely for low Ω_{mat} cosmologies. Our test will be able to discriminate between low and high Ω_{mat} values. A general characteristic of the contour maps is the tendency to be drawn toward negative values of Λ . This too is expected from Fig.2 where we note the asymptotic regime of the x ratios toward these values. Our test is not able to discriminate between different values of Λ with only 400 QSOs.

5.4. Binning

The effect of binning is shown in Figs. 5.1 to 5.6. First, with a single bin, the test reduces to the global $\langle V/V_{max} \rangle$, and no model at all may be rejected. Only the models with no Big-Bang (up-left of the map) are rejected because they are not computed! As expected, increasing the binning decreases the allowed range in parameter space, until the map becomes noisy and our method to find the minimum entropy no longer applies.

5.5. The seed

In order not to superimpose the effects of varying the seed and cosmological effects, all the previous figures correspond to Monte-Carlo catalogues drawn with the same initial seed. To illustrate the effects of the statistical fluctuations, we show in Figs. 6 the analyses of ten catalogues of the same size and parent cosmology, which correspond to ten different random seeds. The result is that varying the seed changes the form of the probability map, but does not reject the parent cosmological model.

5.6. Sample size and limiting redshift

Of course the larger the sample, the smaller is the probability map at given confidence level and at fixed higher limiting redshift z_2 . This effect is illustrated in Figs. 7.1 to 7.4. Despite the large number of QSOs in the sample, the test is not able to determine Λ . The fact that the test is not very sensitive to Λ comes from the value of $z_2 = 2.2$ which is not deep enough.

Conversely, the higher z_2 , the more efficient is the test versus cosmological parameters. The effect of increasing z_2 at fixed n is shown on Figs. 8.1 to 8.3.

In fact, these figures show that a high- z limited catalogue is very sensitive to the curvature: on Fig.8.3 the contour probability follows very well the iso-curvature line of the model, with only 400 QSOs in the sample!

To illustrate these effects, we give in Table 1 the ranges corresponding to the 2σ (95 %) confidence level for Ω_{mat} and Ω_k respectively. However these results are quite doubtful beyond $z = 2.2$ where we did not modify our models, while it seems that evolution could reverse (see e.g. Hook *et al.* 1995). Fortunately, the evolution governs only the maximum redshift of magnitude-limited quasars, which are a minority (remember Section 4 and see Paper II).

Table 1. 95 % confidence level limits read in Figs. 7 and 8 for Ω_{mat} and Ω_k for a parent cosmology $\Omega_{mat} = 0.6$, $\Omega_k = -0.2$

N	z_1	z_2	$\Omega_{mat} = 0.60$	$\Omega_k = -0.20$
400	0.3	2.2	$\Omega_{mat} = 0.70 \pm 0.50$	$\Omega_k = -0.15 \pm 0.85$
400	0.3	3.5	$\Omega_{mat} = 0.70 \pm 0.50$	$\Omega_k = -0.05 \pm 0.55$
400	0.3	5.0	$\Omega_{mat} = 0.80 \pm 0.6$	$\Omega_k = -0.05 \pm 0.45$
5000	0.3	2.2	$\Omega_{mat} = 0.75 \pm 0.35$	$\Omega_k = -0.1 \pm 0.5$

We combined the last two results to look for the most efficient use of telescope time dedicated to cosmological tests based on quasars (see Section 7).

5.7. Biasing

5.7.1. Biasing due to lensing

At given redshift, a presumably small, but still unknown, fraction of QSOs are amplified while the other ones are deamplified. The probability that a (lens) galaxy lies closer to the line-of-sight of a given quasar than some threshold sufficient to induce gravitational amplification increases with increasing quasar redshift. As amplified quasars enter preferentially magnitude-limited samples, the result of lensing is to mimic intrinsic luminosity evolution. Unfortunately, we do not know the respective contributions of intrinsic and extrinsic biasing to the observed evolution. As the evolution law we use is purely phenomenological, and not the prediction of e.g. a physical model of the emission in the environment of a massive black hole, it can fit the effects of lensing as well - or as badly - as those of an intrinsic luminosity evolution.

5.7.2. Clustering

Our test relies on the null hypothesis of uniform spatial distribution, which is in principle not compatible with clustering, if any. In fact it is negligible here since our working scale is of the order of the Gpc, and only a weak clustering scale of 40-100 Mpc seems to be detected (Clowes and Campusano 1991, Shanks *et al.*, 1994, Georgantopoulos *et al.*, 1994).

5.7.3. Biasing in z

In order to be as realistic as possible, samples with a deficiency of objects in various redshift ranges have been used. According

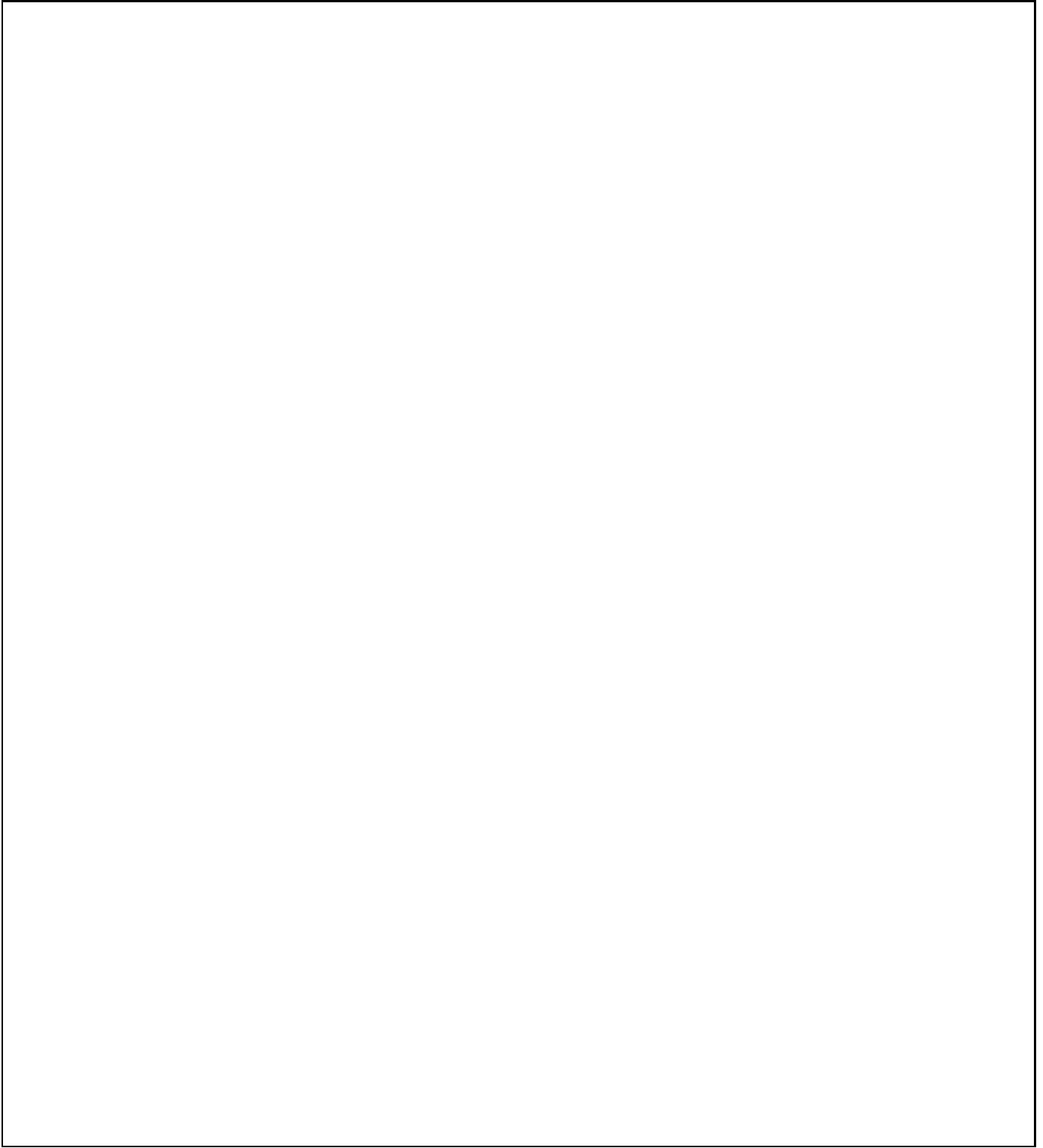


Fig. 4. Contour probability maps varying the parent cosmological model of Monte–Carlo catalogues. Significance levels are 0.1, 1.0, 5.0 and 10 %. All five models are constructed under PWLE with 400 QSOs and the redshift range $[0.3, 2.2]$. They are analysed either under PWLE (left column) or under LEXP (right column). From top to bottom, the models are: $(\Omega_{mat} = 0.0, \Lambda = 0.0, k_L = 2.95)$; $(\Omega_{mat} = 1.0, \Lambda = 0.0, k_L = 3.60)$; $(\Omega_{mat} = 0.0, \Lambda = 1.0, k_L = 1.91)$; $(\Omega_{mat} = 1.0, \Lambda = 1.0, k_L = 3.82)$; $(\Omega_{mat} = 2.5, \Lambda = 1.0, k_L = 4.12)$. Note the strong difference between the probability maps for the low (< 0.2) and high (> 0.2) Ω_{mat} .

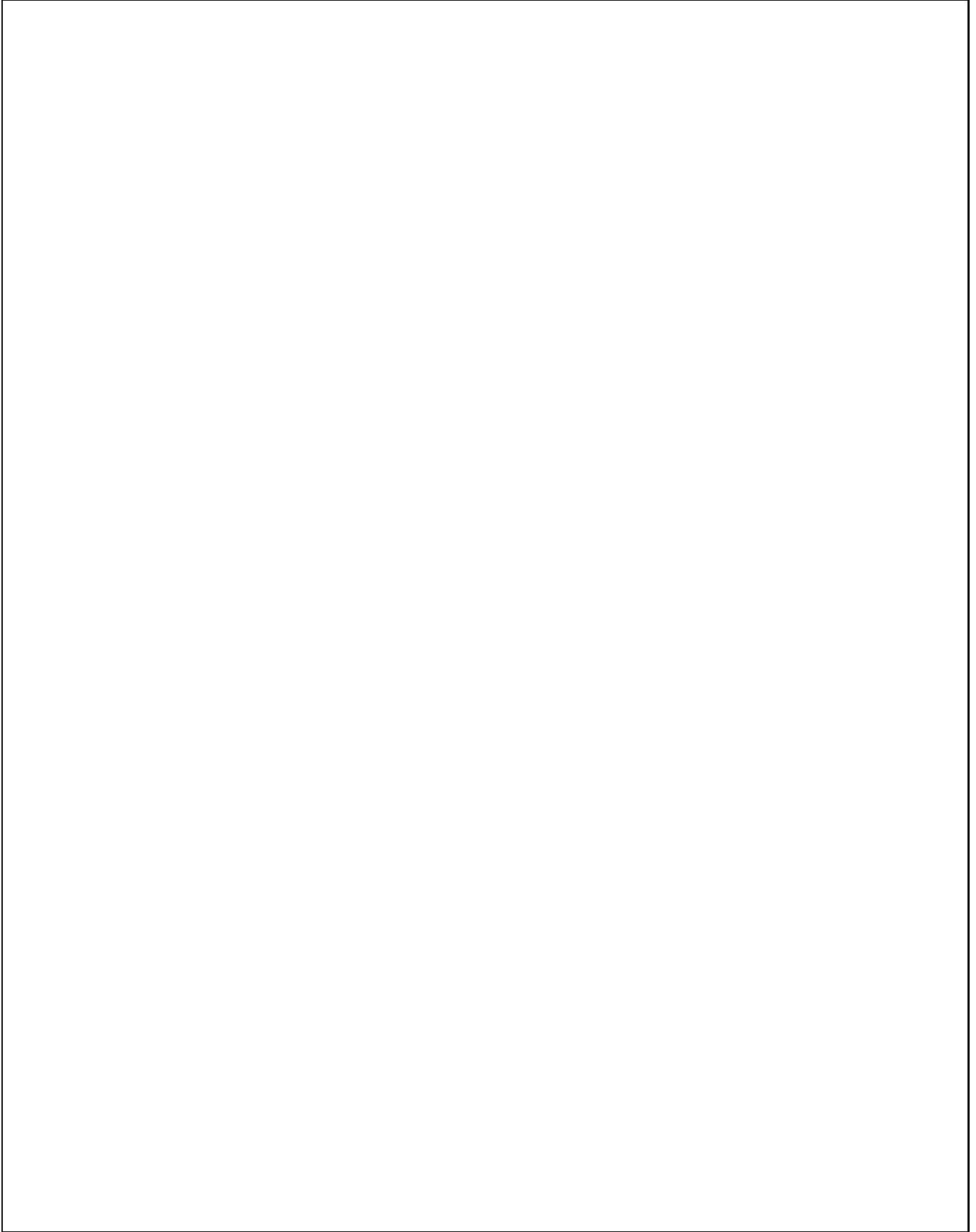


Fig. 5. Same as Fig. 4, varying the binning. A PWLE simulated catalogue ($\Omega_{mat} = \Lambda = 0.6, k_L = 3.47$) of 400 QSOs, with a redshift range of $[0.3, 2.2]$ is analysed under PWLE hypothesis, according to different binnings. From left to right and top to bottom, the number of QSOs per bin is 400, 100, 50, 40, 27, 16.

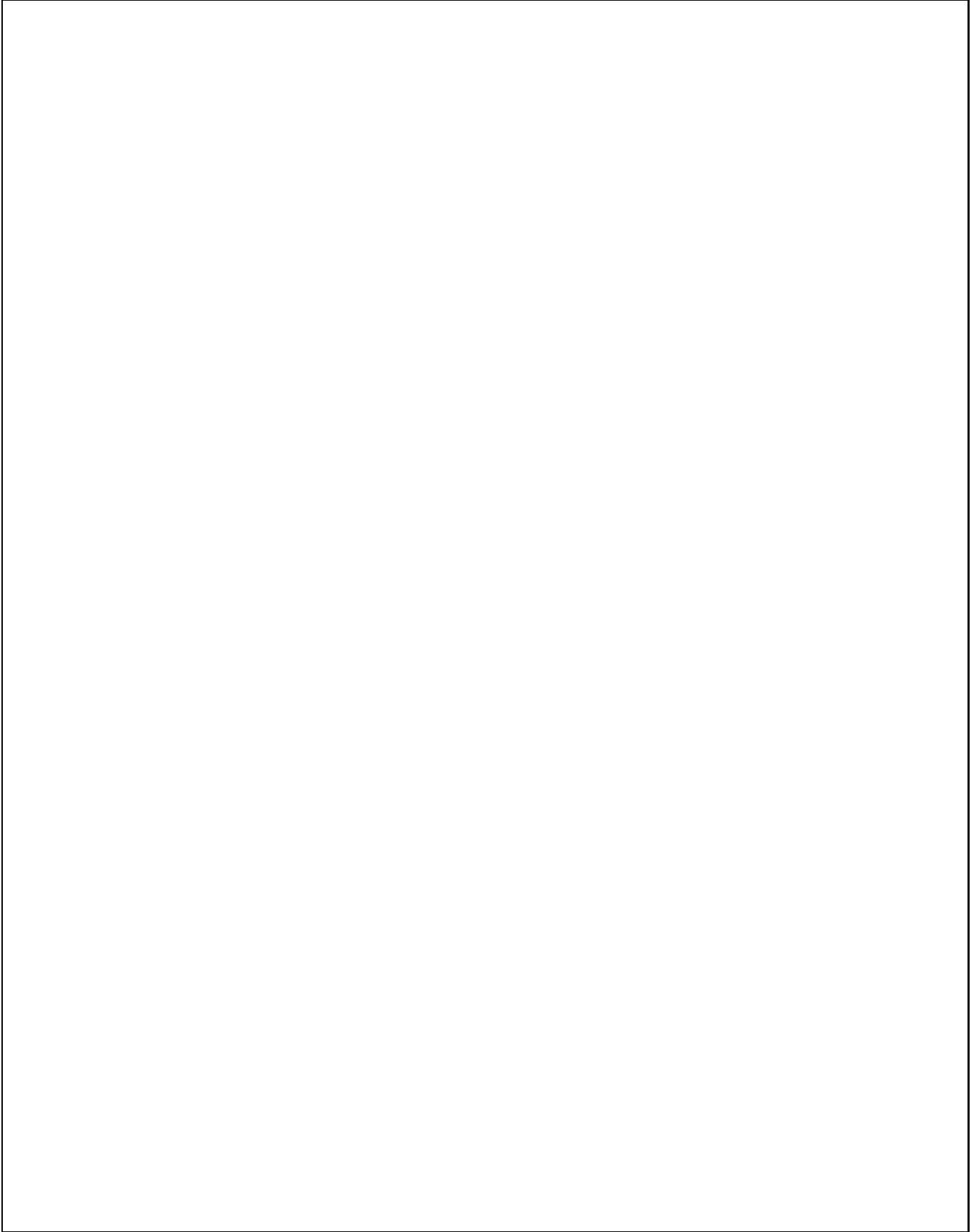


Fig. 6. Same as Fig. 4, varying the seed. Ten different PWLE simulated catalogues in the same cosmological model ($\Omega_{mat} = 0.6$, $\Lambda = 0.6$, $k_L = 3.47$) are analysed under PWLE hypothesis. All catalogues contain 400 QSOs in the redshift range $[0.3, 2.2]$, only the random number seed is different in each catalogue.

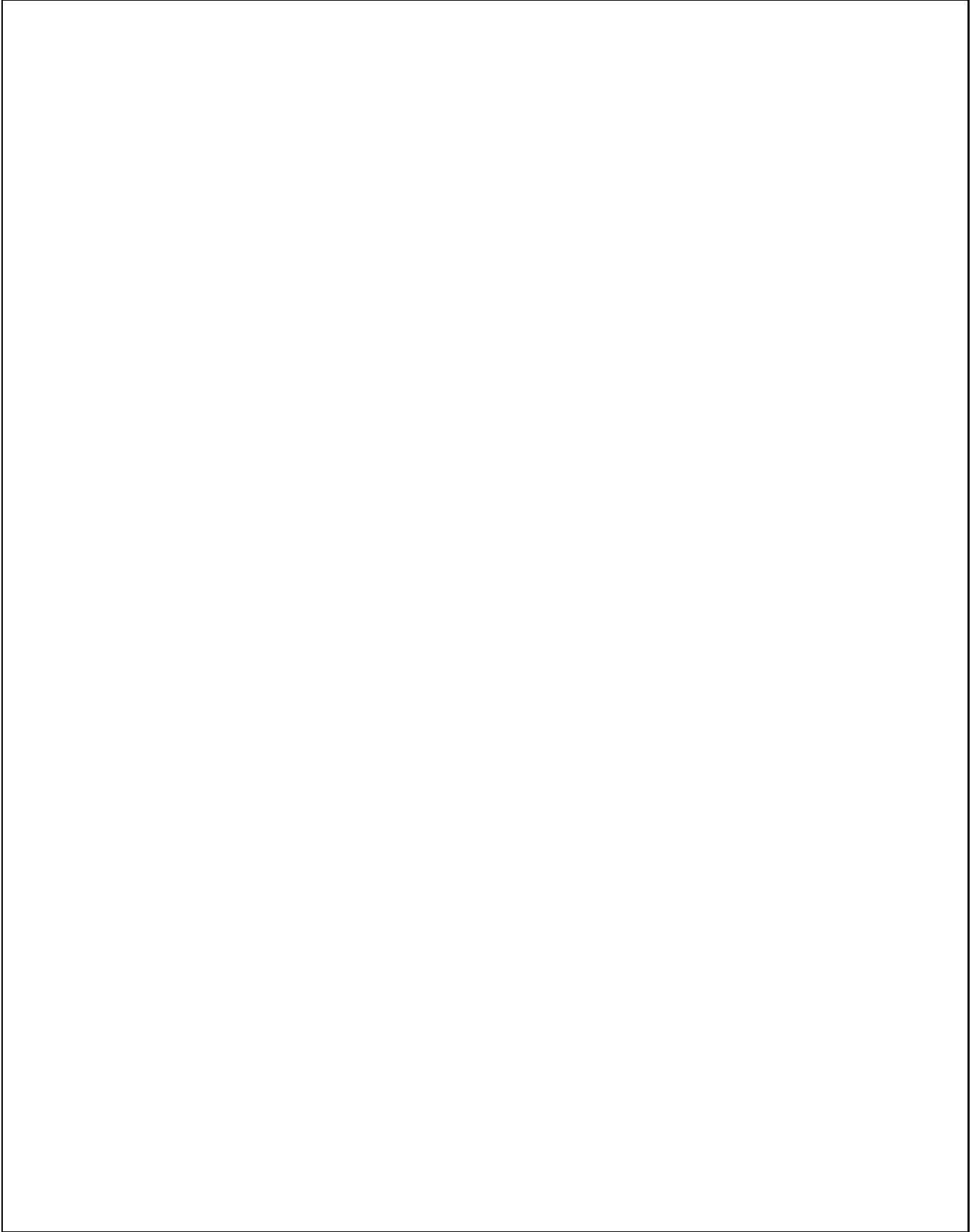


Fig. 7. Same as Fig. 4, varying the catalogue size n . Four PWLE simulated catalogues in the same model ($\Omega = \Lambda = 0.6, k_L = 3.47$), the same redshift range $[0.3, 2.2]$ are analysed under PWLE hypothesis. The values of n are 400, 1000, 3000, 5000 QSOs from top to bottom and from left to right.

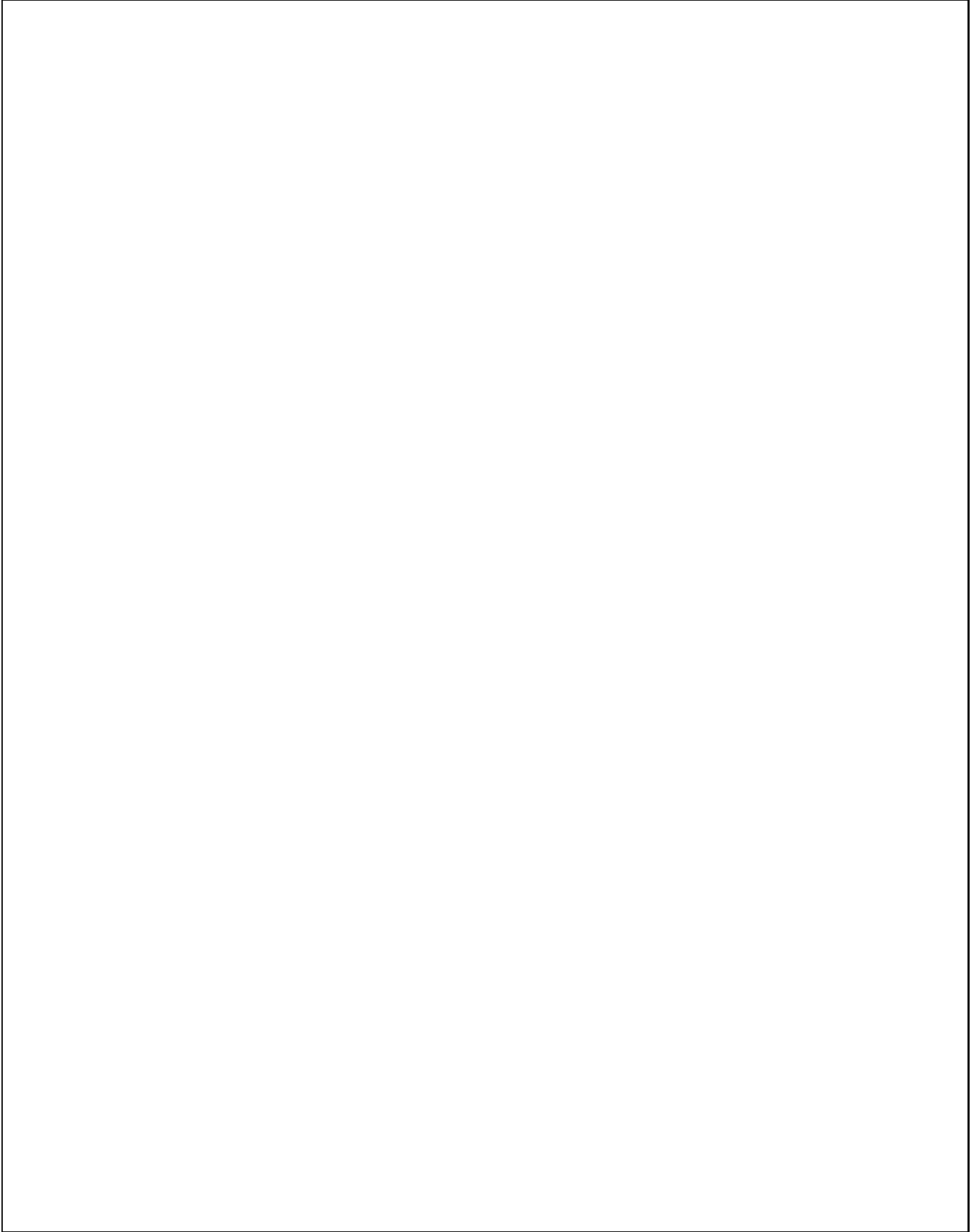


Fig. 8. Same as Fig. 4, varying the upper redshift limitation of the catalogue. Three PWLE simulated catalogues with 400 QSOs, in the same model ($\Omega = \Lambda = 0.6, k_L = 3.47$) are analysed under PWLE hypothesis. The lower redshift is always $z_1 = 0.3$, and the three values of the upper redshift are $z_2 = 2.2, 3.5, 5.0$.

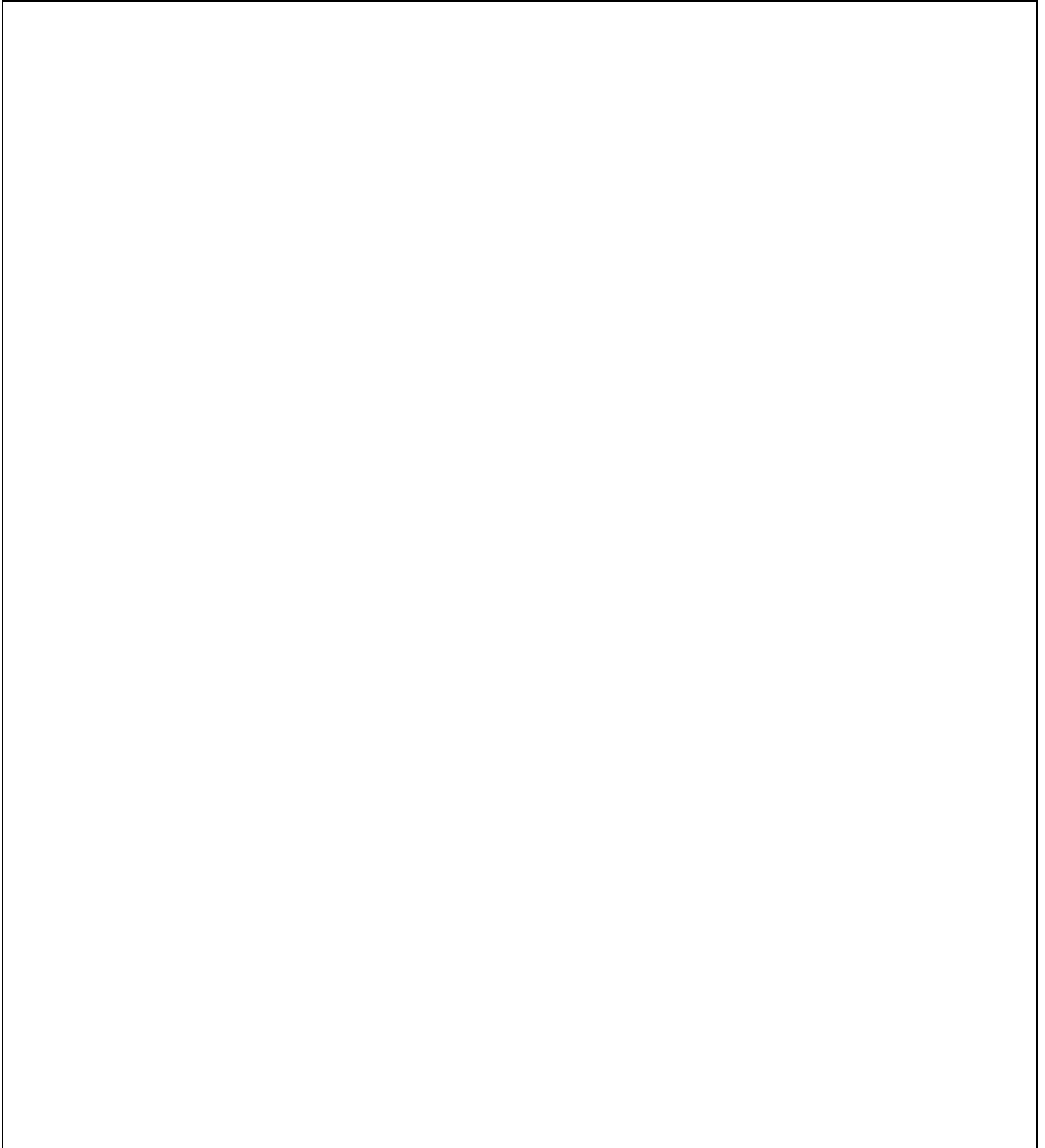


Fig. 9. Effects of the redshift and magnitude biases. The unbiased catalogue contains 546 QSOs, PWLE, in the model $\Omega = \Lambda = 0.6, k_L = 3.47$, and the redshift range $[0.3, 2.2]$. All analyses are done under PWLE hypothesis. The first map (Fig. 9.1) is the analysis of the unbiased simulated catalog. In the top right map, 30% of the QSOs in the redshift range $[0.5, 0.9]$ are subtracted. In the middle left map 30% of the QSOs in the redshift range $[1.5, 1.8]$ are subtracted. In the fourth map the last two redshift biases are present. In the fifth map only a gaussian noise in magnitude, of mean 0.0 and deviation 0.01, and a second component of mean 0.2 and deviation 0.2 has been done. The last map contains all the previous biases.

to Boyle *et al.* (1987; see also Véron 1983), the combination of the run of color versus redshift with a pre-selection based on UV excess results in a deficiency around 30% of objects in the redshift range $0.5 < z < 0.9$. We analysed samples with such a random depletion in this range. We also studied the effects of a similar deficiency in the range $1.5 < z < 1.8$. Figs. 9.2, 9.4, and 9.6 show the effect of this deficiency, which clearly results in a general enlargement of the probability map. Fortunately we have not detected a strong shift of the contour probabilities.

5.7.4. Biasing in magnitude

The photometric biasing has been analysed. We introduced a gaussian noise of mean 0.00 and standard deviation 0.01 mag. To mimic QSO variability, a second component of mean 0.2 and standard deviation 0.2 has been added (Giallongo *et al.* 1991). In Fig. 9.3 there is no redshift bias, but the two photometric biases are included, and Fig. 9.5 has been drawn with the two redshift biases plus the two photometric biases. The absence of strong differences with the non-biased map (Fig. 9.1) shows that the x ratios of the \mathcal{D} QSOs do not depend on their magnitude. Fig. 9.5 shows a map enlarged from Fig.9.1, which is the expected effect caused by any bias.

6. Real QSO Samples

6.1. Application to real quasars

We now apply the test to the sample of 400 UVX quasars of Boyle *et al.* (1990). This sample is based on fiber FOCAP spectroscopy of 1409 UVX objects selected through COSMOS photometry in eight high-latitude Schmidt fields. The limiting B magnitudes and $U - B$ color indices are given in Boyle *et al.*'s Table 2 (1990).

Boyle *et al.* (1988) show that the best fit to the data in this sample is obtained with Pure Luminosity Evolution (PLE) models, far better than PDE. The favoured functional form for LE seems to be a power law (PWLE) rather than an exponential (LEXP).

Both evolution models depend on a single parameter k_L (see Section 2). Fig. 10 gives the probability map obtained with PWLE and LEXP, which appear to be essentially similar. Restricting ourselves to the $\Lambda > 0$ half plane, we discuss the results at the 95 % confidence level:

1) Regarding the matter term, we find, from Fig. 10.a,b that $0.3 < \Omega_{mat} < 1.3$ (PWLE) and $0.2 < \Omega_{mat} < 2$. (LEXP). The minimum entropy in both models is the same and the corresponding probability is 52%. More interestingly, the two functional forms (power law and exponential) lead to similar probability maps, which was expected from the analysis of the simulated catalogues.

2) In Fig. 10.c,d,e,f the two probability maps obtained at low- ($0.3 < z < 1.5$) and high- ($1.5 < z < 2.2$) redshift respectively are compared. The latter range does not allow any rejection among cosmological models, although the 'cosmological signal' is believed to increase with redshift. This is due to the narrowness of the redshift range which does not allow one to discriminate cosmologies, and to the poor sample size (only 112 high- z QSOs). The low-redshift map leads to the following constraint: $\Omega_{mat} < 0.7$ (PWLE) and $\Omega_{mat} < 0.9$ (LEXP). As expected from simulated catalogues, at low redshift range, the test is not sensitive to Λ .

3) Concerning the space curvature, the limits are the following. With QSOs over the entire redshift range $[0.3, 2.2]$ we read from Fig. 10.a,b: $-1.1 < \Omega_k < 0.7$ (PWLE) and $-1.1 < \Omega_k < 0.8$ (LEXP). In the redshift range $[0.3, 1.5]$ we find from Fig. 10.c,d,e,f: $-0.7 < \Omega_k < 1$. (PWLE), and $-0.8 < \Omega_k < 1..$

The constraint on the cosmological constant is only $\Lambda < 1.4$ for both evolution models.

It does not make sense to multiply the probability map of the low- z sample with that obtained from the entire sample because the samples are not independent. However we can restrict the space parameter to the intersection of the space parameter given from these two samples. The results are summarized in Table 2. The 1σ confidence levels are given in Table 3.

Table 2. 95 % confidence limits on Ω_{mat} , Ω_k , and q_0 from low- z and all QSOs together

	$0 < \Lambda < 1.4$	
	PWLE	LEXP
Ω_{mat}	0.5 ± 0.2	0.55 ± 0.35
Ω_k	0.0 ± 0.7	0.0 ± 0.8
q_0	-0.25 ± 1.0	-0.2 ± 1.3

The Luminosity Functions derived from the sample and the estimation of the characteristic evolution times in best models are given in Paper II.

Table 3. 68 % confidence limits on Ω_{mat} , Ω_k , and q_0 from low- z and all QSOs separately

	$0.3 < z < 2.2$	
	PWLE	LEXP
Ω_{mat}	0.75 ± 0.35	0.55 ± 0.25
Ω_k	-0.05 ± 0.65	-0.15 ± 0.55
q_0	0.1 ± 1.2	-0.3 ± 0.9
	$0.3 < z < 1.5$	
	PWLE	LEXP
Ω_{mat}	0.2 ± 0.2	0.25 ± 0.25
Ω_k	0.35 ± 0.65	0.25 ± 0.75
q_0	-0.35 ± 1.0	-0.4 ± 1.1

7. Summary and Discussion

7.1. Summary

There are several points to recall before discussing the results found in Sections 5 and 6.

All the numerical codes we have designed for the present work have been duplicated, independently by two of us, in order to avoid computational errors.

None of the steps of the entire test procedure depends on the Hubble constant H_0 . The test is completely independent of any absolute magnitude or distance scaling, since it only relies on volume ratios and on flux ratios. So, the only parameters

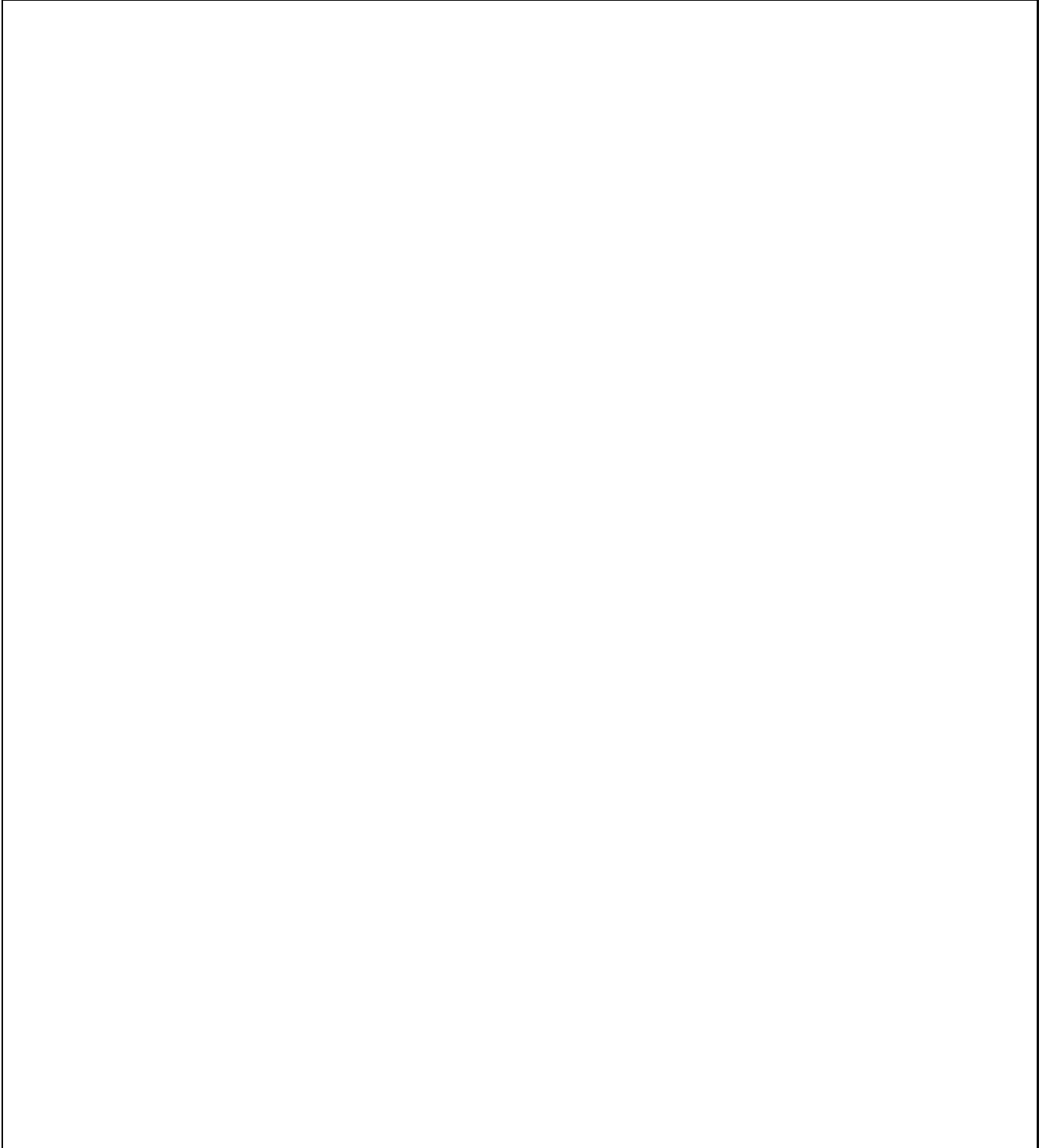


Fig. 10. Contour probability maps (0.1, 1.0, 5.0 and 10 % significance level from outside to center) of the Boyle catalog. Left (right) column is the PWLE (LEXP) analysis. At the top: the whole redshift range $[0.3, 2.2]$, in the middle: the restricted low-redshift range $[0.3, 1.5]$, and in the bottom: the high-redshift range $[1.5, 2.2]$. The latter range is too small to give useful limitations.

which do depend on the choice of H_0 are the characteristic evolution time and the quasar absolute luminosities such as Φ_* , the normalization of the luminosity function given in Paper II. Schade and Hartwick 1994, on the contrary, need an explicit value of Φ_* , thus a choice of H_0 . They also make use of the same functional form and parameters for the luminosity function in all cosmological models. Even if the values used are within error bars for all models, they are better suited to one or more peculiar model, which is likely to bias this test.

Our results on the cosmological parameters only apply *under specific hypotheses concerning quasar evolution*. Such hypotheses are difficult to avoid and the hypotheses made here are quite widely encountered. The present paper is entirely devoted to the case for Luminosity Evolution, which has been favoured by recent studies (Boyle et al. 1988, 1990). There is a way to test the adopted evolution laws: applying the $\langle V/V_{max} \rangle$ test in various redshift bins, and comparing the values found for k_L . Such a procedure however requires quite a large sample. Applying the test in the frame of Density Evolution will be the subject of a forthcoming paper. Quite interesting are the results of cross-tests of the two standard functional forms: samples issued from a simulation with power law (PWLE) and tested with exponential (LEXP) lead to similar probability maps in the (Ω_{mat}, Λ) plane, which makes us rather confident on their generality. Hopefully, such similarities may be expected from cross-tests between Density and Luminosity Evolutions, which will follow in a forthcoming paper. The test seems to be insensitive to the cosmological constant. In fact we showed it is sensitive to a certain function $f(\Omega_{mat}, \Lambda)$ which depends on the redshift depth of the catalogue. $f(\Omega_{mat}, \Lambda) = \Omega_{mat}$ for a catalogue with a low redshift limitation ($z_2 \simeq 2.2$). $f(\Omega_{mat}, \Lambda)$ tends to the curvature $\Omega_{mat} + \Lambda$ for a deep catalogue. By this way, with at least two different catalogues, it is possible to determine Λ . The recent LBQS catalogue of Hewett *et al* (1995), with more than 1000 QSOs, may be useful for this purpose.

7.2. Limits on Ω_{mat} , and the status of Λ

As already underlined, the constraints brought in by the cosmological test described in this paper hold mainly on Ω_{mat} , and to a lesser extent on the curvature term Ω_k ; see Table 2. A low Ω_{mat} is rejected, and we exclude a flat Universe without a cosmological constant. This implies introducing a non zero Λ in the standard inflation models ($\Omega_{tot} = 1$). This is in the sense of the recent determinations of the Hubble parameter which give too low an age for the Universe if $\Lambda = 0$, compared to the age of the oldest stars only (Jaffe, 1995).

Let us compare our limits on Ω_{mat} to what is found in the current litterature, arising from tests of different nature and/or on different scales: The limits coming from velocity fields in voids are obtained without assumptions regarding either the galaxy biasing, Λ , or the fluctuation statistics (Dekel and Rees 1994).

White *et al.* (1993) express Ω_{mat} in terms of f_b , the baryon fraction in clusters of galaxies: $\Omega_{mat} < 0.3 \left(\frac{\Omega_b}{0.06} \right) \left(\frac{0.2}{f_b} \right)$, if the ratio of baryonic to total matter in clusters is representative of the universe. Accounting for the limits on the baryon fraction deduced from X-Ray observations of the Coma cluster, $f_b = 0.009 + 0.05h^{-3/2}$, and on the limits on Ω_b from standard Big-Bang Nucleosynthesis: $0.009h^{-2} < \Omega_{baryon} < 0.02h^{-2}$, we finally get: $\Omega_{mat} < 0.4 \frac{h^{-1/2}}{1+0.18h^{3/2}}$. Comparing our results with

two recent papers is of particular interest: Bernardeau *et al.* (1995) fix $\Omega > 0.3$ at the 2σ level and favour $\Omega = 1$ from the skewness of the cosmic velocity field divergence. Meanwhile Hudson *et al.* (1995), by comparing the distribution of optical galaxies with the POTENT mass distribution, conclude that $\beta = \Omega^{0.6}/b = 0.74 \pm 0.13$ (1σ), favouring either $\Omega = 1$, $b = 1.35 \pm 0.23$ or $b = 1$, $\Omega = 0.6 \pm 0.18$. Cole *et al.* (1995) describe similar work from IRAS redshift surveys and find that $\beta = 0.5 \pm 0.2$, implying $\Omega = 1$, $b \simeq 2$ or $b = 1$, $\Omega = 0.35$. This last two results are surprisingly close to ours: $\Omega = 0.5 \pm 0.2$ (2σ) (PWLE) or $\Omega = 0.55 \pm 0.3$ (2σ) (LEXP). Perhaps we can conclude that the bias parameter b is of order unity, but this still appears to be premature!

All these results are summarized in Table 4.

The test described in the present paper, performed with QSOs, measures the cosmological parameters on a scale of several *Gpc*. It agrees well with most of the tests given in Table 4. The only exception concerns the results on the centers of clusters of galaxies (both the Virial Theorem and the Giant Arcs) which have been operated on smaller scales, typical of structures which have detached from the general expansion, then collapsed and dissipated. Furthermore, these tests rely on the assumption of a universal Mass to Light ratio, and it is not surprising to find smaller Ω_{mat} on smaller scales.

7.3. Optimal strategy for quasar detection aimed at cosmology

We combined the results of the last two series of simulations to look for the most efficient use of telescope time aimed at cosmological tests based on quasars. We saw that for the same precision on the cosmological parameters, say Ω_{tot} , about 10 times less QSOs are needed if their limiting redshift is 3.5 instead of 2.2. Let us compare two possible observational strategies for quasar detection, for example with the FUEGOS multifiber spectrograph to be build for the VLT at ESO: first, programme 1, a classical preselection of UVX candidates brighter than $B = 24$ with some limit in $U - B$, and second, programme 2, consisting off the spectroscopy of all stellar or compact objects brighter than $R = 23$ (Mathez *et al.*, 1995a). A selection of $I < 22.5$ could be preferred. A preselection of UVX candidates (or simply through the blue filter, see Glazebrook *et al.* 1995) will be efficient with a QSO/candidates ratio around 1/3. The drawback, however, is the redshift limitation inherent in the blue selection. In programme 2, the drawback is that the *QSO/candidate ratio* is far (to what extent ?) lower. The question is wether this drawback may be compensated by the higher limiting redshift, which would be higher than 2.2. The last source of error is that we used a simulated catalogue with an evolution extrapolated from low redshifts to $z = 3.5$. Although the evolution law at these high redshifts is unknown, it is probably different from the evolution at low redshift. The two strategies are compared in Table 4, note however that many input quantities in Table 4 are only first guesses. The surface density $\Sigma = 300 \text{ deg.}^{-2}$ of QSOs brighter than $B = 24$ is one of the most secure inputs (to within a factor of 2) since convergent results have been found by Glazebrook *et al.* (1995) and Koo, Kron and Cudworth (1986). The QSO/candidate ratio expected in programme 2 was taken as 1/30 to compare the two programmes. We think that it is rather conservative for a selection through the red filter and is likely to allow a higher limiting redshift. The quasar evolution at redshifts above 2.5 is

Table 4. Limits on Ω_{mat} obtained in various recent tests

Test	Ω	confidence level	Λ	reference
Galaxies:				
Sp - H.	$0.1 < \Omega < 1$	1.5σ	$\Lambda = 0$	Zaritsky and White (1993)
Clusters:				
CoG: VT	$\Omega h_{75}^{-1} = 0.2 \pm 0.1$		$\forall \Lambda$	
CoG: Giant Arcs	$\Omega h_{75}^{-1} = 0.2 \pm 0.1$		$\Lambda=0$	Fort and Mellier (1994)
CoG: Weak Shear	$\Omega h_{75}^{-1} = 1 \pm 0.5$		$\Lambda=0$	Bonnet <i>et al.</i> (1994) Fahlman <i>et al.</i> (1994)
CoG: f_b	$\Omega h_{75}^{1/2} < 0.5$		$\Lambda=0$	White <i>et al.</i> (1993)
Velocity Fields:				
CVT-CfA1	$\Omega = 0.5 \pm 0.1$		$\forall \Lambda$	
POTENT-IPDF	$0.3 < \Omega$	5σ	$\forall \Lambda$	Dekel (1994)
POTENT-VOIDS	$0.3 < \Omega$	2.4σ	$\forall \Lambda$	Dekel and Rees (1993)
POTENT-SKEW	$0.3 < \Omega$	2σ	$\forall \Lambda$	Bernardeau <i>et al.</i> (1995)
QSOs:				
spatial distribution	$\Omega = 0.4 \pm 0.2$	1σ	$\Lambda = 0$	Deng <i>et al.</i> (1994)
Loh-Spillar	$\Omega = 0.2 \pm 0.1$	1σ	$\Lambda = 0$	
	$\Omega = 0.4 \pm 0.1$	1σ	$\Lambda = 1 - \Omega$	Schade <i>et al.</i> (1994)
This Work:	$\Omega = 0.5 \pm 0.2$	2σ	$\Lambda < 1.4$	PWLE
	$\Omega = 0.5 \pm 0.3$	2σ	$\Lambda < 1.4$	LEXP

also questionable. It seems to reverse (Hook *et al.* 1995), but it is not easy to ascertain because of the different observational approaches below and above this redshift. The surface density of stars to 23rd magnitude has been estimated from the model of Robin (1989). As for the surface density of quasars to $R = 23$, Table 4 gives a conservative estimate since no quasar selection has ever been made in R . Recent results by Webster (1994) seem to indicate that red quasars are not rare, and that the surface density of red or infrared QSOS could be far higher.

With the 80 fibres of FUEGOS, both programmes may be expected to have similar global efficiencies for the determination of Ω_{mat} . However they would lead to different scientific outputs: a complete sample of 10,000 QSOs in the first case, allowing excellent statistics for quasar studies, and a better idea of the QSO evolution at high redshift, i.e. presumably constraints on galaxy formation, in the second one. And a good model of high- z evolution is what we need to determine Λ from this test.

Acknowledgements It is a pleasure to acknowledge B. Fort, P.Y. Longaretti, S. Andreon, J. Bartlett, J.F. Le Borgne, L. Nottale R. Pelló, JP Picat, G. Soucail, S. Collin-Souffrin for all the enlightening discussions we had on QSOs and cosmology, and especially T. Bridge for a careful reading of the manuscript. L.V.W. thanks the french MESR for grant 93135. This work was supported by grants from the french CNRS (GdR Cos-

Table 5. Optimal strategy for detection of quasars with FUEGOS with 80 fibres (FF= FUEGOS FIELD = 1/7 sq. deg.)

	$U - B < 0.2$	No Preselection
m_{lim}	B=24	R=23
$\Sigma_{cand} (deg^{-2})$	1050	7500
$\Sigma_{QSO} (deg^{-2})$	300	250
QSO/candidate	1/3.5	1/30
candidate/FF	150	1100
QSO/FF	50	35
exposures/FF (80 fb)	2	14
$N_{QSO} (\sigma_{\Omega_k} = 0.5)$	5000	400
survey area (deg^2)	17	1.6
FF	100	12
total exposures	200	170

mologie), from the European Community (Human Capital and Mobility ERBCHRXCT920001).

8. References

- Alcock, C., Paczynski B., 1979, MN 281, 358
Avni, Y., Bahcall J., 1980, ApJ 235, 694

- Bernardeau, F., Juszkiewicz, R., Dekel, A., Bouchet, F., 1995, MNRAS 274, 20
- Bigot, G., Triay, R., 1991, Phys. Let. A 159, 201
- Bonnet, H., Mellier, Y., Fort, B., ApJ 427, L83
- Boyle, B.J., Fong, R., Shanks, T., Peterson B.A., 1987, MN 227, 717
- Boyle, B.J., Shanks, T., Peterson B.A., 1988, MN 235, 935
- Boyle, B.J., Fong, R., Shanks, T., Peterson B.A., 1990, MN 243, 1
- Broadhurst, T., Ellis, R., Koo, D., Szalay, A., 1990, Nature 243, 726
- Carroll, S.M., Press, W.H., Turner, E.L., 1992, Ann. Rev. of A& A 30, 499
- Crawford, D.F., 1995, ApJ 441, 488
- Dekel, A., 1994, Ann. Rev. A. & A 32, 371
- Dekel, A., Rees, M., 1994, ApJ 422, L1
- Deng, Z., Xia, X., Fang, L.Z., ApJ 431, 506
- Efron, B., 1979, Ann. Statist. 7, 1
- Fahlman, G.G., Kaiser, N., Squires, G., Woods, D., 1994 ApJ 437, 56
- Fort, B., Mellier, Y., 1994 A& A Rev. 5, 239
- Freedman, W.L., Madore, B.F., Mould, J.R., Hill, R., Ferrarese, L., Kennicutt Jr. R.C., Saha, A., Stetson, P.B., Graham, J.A., Ford, H., Hoessel, J.G., Huchra, J., Hughes, S.M., Illingworth G.D., 1994, Nature 371, 757
- Giallongo, E., Trevese, D., Vagnetti, F., 1991, ApJ 377, 345
- Glazebrook, K., Ellis, R., Colless, M., Broadhurst, T., Allington-Smith, J., Tanvir, Nial, 1995, MNRAS 273, 157
- Hawkins, M.R.S., Stewart, N.J., 1981, ApJ 251, 1
- Helbig, P., Kayser, R., 1995, SISSA preprint
- Hewett, P.C., Foltz, C.B., Chaffee, F.H., 1995, Astron. J. 109, 4, 1498
- Hook, I.M., McMahon, R.G., Patnaik, A.R., Browne, I.W.A., Wilkinson, P.N., Irwin, M.J., Hazard, C., 1995 MNRAS 273, L63
- Hudson, M.J., Dekel, A., Courteau, S., Faber, S.M., Willick, J.A., MNRAS 274, 305
- Kassiola, A., Mathez, G., 1991, AA 230, 255
- Kochanek, C.S., 1992, ApJ 384, 385
- Jaffe, A., 1995, SISSA preprint
- Jing, Y.P., Mo H.J., Börner, G., Fang, L.Z. MNRAS: SISSA preprint
- Lampton, M., Margon, B., Bowyer, S., 1976, ApJ 208, 177
- Leonard, S., Lake, K., 1995, SISSA preprint
- Llorente, A., Pérez-Mercader, J., 1995, SISSA preprint
- Loh, E.D., Spillar, E.J., 1986, ApJ 307, L1
- Malhotra, S., Turner, E.L., 1994, SISSA preprint
- Marshall, H.L., Avni, Y., Braccisi, A., Huchra, J.P., Tananbaum, H., Zamorani, G., Zitelli, V. 1984, ApJ 283, 50
- Mathez, G., 1976, AA 53, 15
- Mathez, G., 1978, AA 68, 17
- Mathez, G., Kassiola, A., Lachièze-Rey, M., 1991, AA 242, 13
- Mathez, G., Mellier, Y., Picat, J.P., 1995a, proceedings of "Science with the VLT", ESO Workshop, J. Walsh ed., Munich 1994.
- Mathez, G., Van Waerbeke, L., Bonnet, H., 1995b submitted (Paper II),
- Nottale, L., 1993, Fractal Space-Time and Microphysics, chpt 7, World Scientific ed.
- Phillipps, S., 1994, MN 269, 1077
- Pierce, M.J., Welch, D.L., McLure, R.D., van den Bergh, S., Racine, R., Stetson, P.B., 1994, Nature 371, 385
- Press, W.H., Teukolsky, S.A., Vetterling, W.T., Flannery, B.P., 1992, Numerical Recipes, Cambridge University Press, p.686
- Primack J.R., 1995, SISSA preprint
- Robin, A., 1989, PhD. dissertation, Université de Besançon
- Schade, D., Hartwick F.D.A., 1994, ApJ 423, L85
- Schmidt, M., 1968, ApJ 151, 393
- Schmidt, M., 1972, ApJ 176, 273
- Schmidt, M., Green, R.F., 1983, ApJ 269, 352
- Shanks, T., Boyle, B.J., 1994, MN 271, 753
- Shaver, P.A., "High Redshift Quasars", to appear in *17th Texas Symposium on Relativistic Astrophysics and Cosmology*, Böhringer et al. eds, Ann. New York Academy of Science
- Turner, E.L., 1979, ApJ. 230, 291
- Van den Bergh, S., 1994, PASP 106, 1113
- Véron, P., 1983, Proc. 24th Liège Astrophys. Col. 'Quasars and Gravitational Lenses', Institut d'Astrophysique, Univ. de Liège, p.210
- Véron-Cetty, M.P., Véron, P., 1991, ESO Scientific Report, p.8
- Webster, R., 1994, XXIIInd IAU General Assembly, The Hague.
- Weinberg, S., 1989, Rev. Mod. Phys. 61, 1
- Yoshii, Y., Peterson, B.A., 1995, ApJ 444, 15
- Zaritski, D., White, S.D.M., 1993, ApJ 405, 464
- Zieba S., Chyzy K., 1991, AA 241, 22